



ELSEVIER

Available online at [www.sciencedirect.com](http://www.sciencedirect.com)

SCIENCE @ DIRECT®

Deep-Sea Research I 51 (2004) 1229–1244

DEEP-SEA RESEARCH  
PART I

[www.elsevier.com/locate/dsr](http://www.elsevier.com/locate/dsr)

# Photosynthesis and light regime in the Azores Front region during summer: are light-saturated computations of primary production sufficient?

Luisa M. Lorenzo<sup>a,\*</sup>, Francisco G. Figueiras<sup>a</sup>, Gavin H. Tilstone<sup>b</sup>,  
Belén Arbones<sup>a</sup>, Iván Mirón<sup>a</sup>

<sup>a</sup> CSIC, Instituto de Investigaciones Mariñas, Eduardo Cabello 6, 36208 Vigo, Spain

<sup>b</sup> Plymouth Marine Laboratory, Prospect Place, West Hoe, Plymouth PL1 3DH, UK

Received 21 January 2003; received in revised form 7 October 2003; accepted 13 January 2004

## Abstract

Bio-optical variables for primary production (PP) computations were determined at the Azores Front (AF) (30–38°N to 20–23°W) between 30 July and 21 August 1998. The area was characterized by the presence of a deep chlorophyll maximum (DCM) at ~100 m and by high mesoscale variability in surface waters caused by the meandering eastern flow of the Azores Current associated with the AF. The vertical distribution of the photosynthetic parameters was typical of oligotrophic waters with high values of light-limited slope ( $\alpha^B$ ) and maximum quantum yield ( $\phi_m$ ) at the DCM and high values of the chlorophyll-specific maximum photosynthetic rates ( $P_m^B$ ) at the surface. Spatial variability in photosynthetic parameters at the surface was high and comparable to that over larger spatial scales. Photosynthetic parameters at the surface associated with contrasting hydrographic structures were significantly different but at the DCM no significant differences were apparent. Although comparisons between the light absorbed by phytoplankton ( $E_{zPUR}$ ) and the corresponding spectral light saturation parameters ( $E_{kPUR}$ ) indicated that photosynthesis was light-limited during sunrise and sunset, integrated PP could be estimated using a simple light-saturated model (DLS model) that considers the day length equivalent for saturating irradiance of photosynthesis and the vertical distribution of  $P_m^B$  and chlorophyll concentration. This means that PP computations for modeling could be greatly simplified by ignoring the spectral resolution and suggest that efforts in further research should be directed to characterize time and spatial variations of  $P_m^B$  in these oligotrophic waters.

© 2004 Elsevier Ltd. All rights reserved.

**Keywords:** Photosynthesis; Light regime; Primary production; Azores Front

## 1. Introduction

Although it is generally assumed that photosynthesis at the deepest layers of the photic layer in

\*Corresponding author. Tel.: +34-986-231930; fax: +34-986-292762.

E-mail address: [luimar@iim.csic.es](mailto:luimar@iim.csic.es) (L.M. Lorenzo).

oligotrophic oceanic regions with a deep chlorophyll maximum (DCM) is light-limited, very few detailed studies on this topic have been made until now (Morel et al., 1996). Light limitation is frequently suggested because of the low light found and the associated photosynthetic response of phytoplankton at these depths, such as high maximum quantum yields, low light saturation parameter values and photo-inhibition when phytoplankton is exposed to higher irradiances.

Because of these photo-physiological characteristics, spectral models are usually applied to estimate primary production (PP) from photosynthesis–irradiance relationships at these oceanic regions (e.g. Morel, 1991; Morel et al., 1996; Keywalyanga et al., 1992; Bouman et al., 2000b). These models, which involve considerable computational time and effort, also require accurate estimates of the spectral photosynthetic parameters and precise characterization of the spectral light field is also needed. By contrast, more simple light-saturated models that only need information about photo-period, horizontal and vertical distributions of chlorophyll and light-saturated rate of photosynthesis ( $P_m^B$ ), could be advantageous (e.g. Behrenfeld and Falkowski, 1997a, b). Moreover, while modeling  $P_m^B$  looks promising (Behrenfeld et al., 2002a, b), accurate prediction of  $\phi_m$  is more difficult (Babin et al., 1996). However, before light-saturated models can be used with sufficient accuracy, it is necessary to assess the extent to which photosynthesis is light-limited in the water column in these regions. If light limitation is negligible, the spectral resolution of calculating PP can be ignored without reducing accuracy.

The Azores Front (AF), which is located at the northern boundary of the North Atlantic subtropical gyre, is an oligotrophic region with enough spatial heterogeneity to assess the degree of light limitation and the photosynthesis response.

The AF is associated with the Azores Current (AC) (Gould, 1985; Siedler et al., 1985), which originates in the transition zone between the Gulf Stream and the North Atlantic Current (Fig. 1) and flows eastward at  $\sim 34^\circ\text{N}$  (Klein and Siedler, 1989). The AF and the meandering circulation of

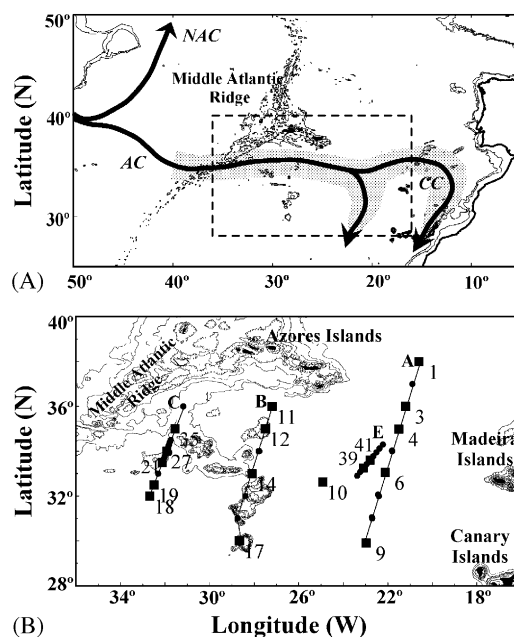


Fig. 1. Schematic representation of the origin and flow of the AC (A) and detailed map of the study area south of Azores Islands (B). In (A) are represented the AC, the Canary Current (CC) and the North Atlantic Current (NAC). The shaded area represents the meanders zone of the AC. Dashed rectangle is the study area. In (B) circles correspond to CTD station and numbered squares to the stations at which additional bio-optical measurements were made.

the AC with its associated eddies (Käse and Siedler, 1982; Pingree, 1997) produce considerable spatial heterogeneity in the hydrographic and biological fields. In addition, the presence of a DCM at  $\sim 100\text{ m}$  depth (Fasham et al., 1985) determines strong vertical patterns in biological and photo-physiological properties (e.g. Cullen, 1982; Babin et al., 1996). Although some of the biological implications caused by this variability in the Azores region has already been described (e.g. Fasham et al., 1985; Kahru et al., 1991; Fernández and Pingree, 1996; González et al., 2001), little attention has been given to the photosynthetic response of phytoplankton (Platt et al., 1983) and bio-optical variability in this region.

In this paper, we present a detailed analysis of the bio-optical variability and the photosynthetic response in the Azores region during summer, which allowed us to investigate whether

photosynthesis was light-limited in the photic layer. Specific attention was given to photosynthesis at the DCM where about a half of total integrated PP of the water column occurred. The performance of a simple light-saturated model for carbon fixation in the region was assessed and compared with the results from spectral estimates.

## 2. Methods

The region between 30–38°N and 20–33°W, south of the Azores Islands (Fig. 1), was visited by R./V. *Hespérides* during summer 1998 (30 July–21 August). Sampling was done along three large-scale latitudinal sections (A–C) centered at approximately 22°W, 28°W and 32°W. Section C was intensively sampled between 34°N and 32°W to better characterize the variability of the zone where the AC penetrates in the region. In addition, a mesoscale section between 34°N and 23°W (section E, Fig. 1) was also sampled. Sampling was performed with a conductivity–temperature–depth (CTD) equipped with fluorometer and rosette with 24 × 121 Niskin bottles.

Bio-optical sampling was conducted at 17 stations (numbered squares in Fig. 1) where photosynthetic parameters, phytoplankton absorption coefficients and spectral light field in the water column were determined. For photosynthetic parameters and phytoplankton absorption coefficients samples were collected around midday from 4 to 6 depths between the surface and the DCM with at least two depths in the upper mixed layer. Additionally, 2–4 samples were taken within the DCM, two in the narrowest DCM profiles and four in the widest. Water samples were collected from the CTD up-cast and immediately transferred to black carboys to prevent light shock, which might have been especially important for the deepest samples.

### 2.1. Chlorophyll and phytoplankton absorption coefficients

Chlorophyll *a* (Chl) concentrations were determined by fluorometry on 250 ml samples after low vacuum pressure filtration through 25 mm What-

man GF/F filters and overnight extraction in 90% acetone. In all, 257 Chl measurements were made from 17 bio-optical stations and a further 16 hydrographic stations. The extracted Chl values were used to calibrate the up-cast fluorescence readings (FR) of the CTD ( $\text{Chl} = 1.53 \times \text{FR} - 0.02$ ;  $r^2 = 0.93$ ), which allowed us to characterize the vertical distributions of Chl along the sections.

Phytoplankton light absorption coefficients ( $a_{\text{ph}}(\lambda)$ ,  $\text{m}^{-1}$ ) were determined by filtering seawater volumes of 2–4 l through 25 mm Whatman GF/F filters. The optical density spectra (400–750 nm) of concentrated particles were measured on board with a dual-beam spectrophotometer at 1 nm bandwidth. A wet filter, moistened with filtered seawater, was used as a blank. The optical density of non-algal material was determined on the same filter after pigment extraction following Kishino et al. (1985). Absorbance at 750 nm was subtracted from all other wavelengths in the spectra and the pathlength amplification was corrected according to Arbones et al. (1996). Although the work by Moore et al. (1995) indicates that the use of general algorithms might lead to overestimates of absorption coefficients when *Prochlorococcus* and *Synechococcus* are dominant, we decided do not apply the specific algorithms for these organisms because, especially for *Prochlorococcus*, the resulting maximum quantum yields were higher than the theoretical maximum for the deepest samples. In addition, absorption coefficients calculated using the algorithm of Arbones et al. (1996) were always less than 2% higher than those estimated using the algorithm for *Synechococcus*.

### 2.2. Irradiance at the sea surface and in the water column

The incident photosynthetic active radiation (PAR) ( $\lambda = 400\text{--}700\text{ nm}$ ) irradiance during the cruise was measured on deck with a Li-190SA cosine-sensor at 1 min intervals and integrated hourly. Fig. 2 shows the mean and standard deviation of PAR irradiance at the sea surface for every hour during the cruise. The coefficient of variation was higher at dawn and dusk ( $\sim 80\%$ ) when incident irradiance was low (mean =  $25\ \mu\text{mol m}^{-2}\text{ s}^{-1}$ ) than at midday ( $\sim 13\%$ ) when

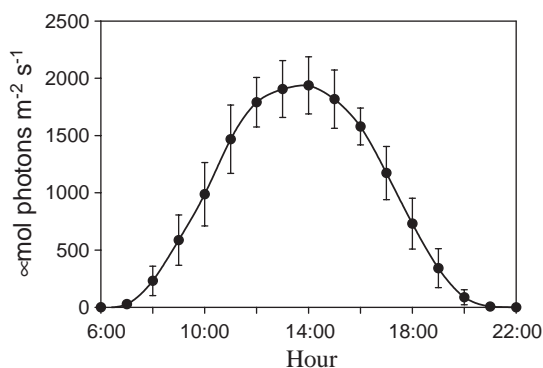


Fig. 2. Hourly mean and standard deviation of the incident PAR at the sea surface during the cruise from 30 July to 21 August 1998.

irradiance was high ( $\sim 1900 \mu\text{mol m}^{-2} \text{s}^{-1}$ ). To remove this daily variability and to facilitate comparisons between stations and regions the hourly average incident irradiance ( $\bar{E}_{0+}(t)$ ,  $\mu\text{mol m}^{-2} \text{s}^{-1}$ ) was considered for all subsequent analysis and PP computations.

The spectral incident irradiance at the sea surface and the downwelling irradiance in the water column were determined with a Licor Li-1800UW spectroradiometer at all bio-optical stations (midday). Measurements in the water column were taken at 1, 10, 20, 40, 60, 80, 100 and 120 m. Additional measurements of incident spectral irradiance at the sea surface were taken along the day light hours during the cruise. To analyze the possible variations in the shape of the incident spectrum along time and place during the cruise, all the incident irradiance spectra  $E_{0+}(\lambda)$  were divided by its integral to obtain the shape, which were compared among them using regression analysis. Spectral shapes showed high correlation ( $0.72 < r^2 < 0.99$ ) with the slopes of the linear regressions varying between 0.993 and 1.007, which indicates that the shape (quality) of incident irradiance spectra did not change significantly along the day and during the cruise. The average normalized incident spectra were compared with the average normalized spectra just below the sea surface. The correlation was also high ( $r^2 = 0.88$ ) and the slope of the linear regression was 0.999, which means that the transmittance through the air–water interface was constant along the spec-

trum wavelengths (Kirk, 1983). This implies that a single spectral shape of incident light can be used for the whole cruise.

The hourly mean spectra just below the sea surface were estimated as

$$\bar{E}_{0-}(t, \lambda) = 0.97 \bar{E}_{0+}(t) \bar{E}_{N0+}(\lambda), \quad (1)$$

where  $\bar{E}_{N0+}(\lambda)$  is the average of the normalized spectra at the sea surface and the constant 0.97 is the transmittance at the air–sea interface (Kirk, 1983).

The scalar spectral irradiance at each hour and depth in the water column was estimated from

$$\bar{E}_z(t, \lambda) = 1.2 \bar{E}_{0-}(t, \lambda) \exp[-K(\lambda)z], \quad (2)$$

where  $K(\lambda)$  ( $\text{m}^{-1}$ ) is the spectral attenuation coefficient estimated from the profiles of downward spectral irradiance at each bio-optical station and 1.2 converts downward irradiance to scalar irradiance (Kirk, 1983).

The hourly spectral irradiance absorbed by phytoplankton at each depth in the water column ( $\bar{E}_{z\text{PUR}}(t)$ ,  $\mu\text{mol m}^{-3} \text{s}^{-1}$ ) is

$$\bar{E}_{z\text{PUR}}(t) = \int_{\lambda=400}^{700} \bar{E}_z(t, \lambda) a_{z\text{ph}}(\lambda) d\lambda, \quad (3)$$

where  $a_{z\text{ph}}(\lambda)$  ( $\text{m}^{-1}$ ) is the phytoplankton spectral absorption coefficient at each depth.

### 2.3. Photosynthesis–irradiance experiments and daily water-column primary production

The photosynthesis–irradiance determinations were carried out in linear incubators illuminated with tungsten–halogen lamps (50 W, 12 V) and refrigerated with thermostatic baths. From each sampling depth 14 subsamples were collected in 75 ml Corning tissue culture flasks and inoculated with  $3.70 \times 10^5$  Bq (10  $\mu\text{Ci}$ ) of  $\text{NaH}^{14}\text{CO}_3$ . For each curve one bottle was covered with aluminum foil and placed at the end of the incubator to check dark carbon fixation. After the incubation time (2–3 h), samples were filtered under low vacuum pressure through 25 mm Whatman GF/F filters and exposed to HCl fumes for 6–12 h to eliminate unincorporated inorganic  $^{14}\text{C}$ . The external standard and the channel ratio methods were used to correct for quenching and determine dpm.

The maximum irradiance used in the incubators varied between  $\sim 1200 \mu\text{mol m}^{-2} \text{s}^{-1}$  for samples from the surface and  $\sim 400 \mu\text{mol m}^{-2} \text{s}^{-1}$  for the deepest samples. The irradiance at each position in the incubator was checked regularly during the cruise with a Li-Cor cosine-sensor LI-190SA. Because the spectral quality of the incident light did not change along the short incubators that were used (see Arbones et al., 2000), the spectral irradiance at each position in the incubators  $E(\lambda)$  was calculated by multiplying the normalized spectrum of the tungsten-halogen lamps  $E_{\text{NL}}(\lambda)$  and the corresponding PAR irradiance at each location (Figueiras et al., 1999; Arbones et al., 2000), where

$$E_{\text{NL}}(\lambda) = E_{\text{L}}(\lambda) / \int_{\lambda} E_{\text{L}}(\lambda) d\lambda \quad (4)$$

and  $E_{\text{L}}(\lambda)$  is the lamp spectrum.

The PAR absorbed by phytoplankton ( $E_{\text{PUR}}$ ,  $\mu\text{mol m}^{-3} \text{s}^{-1}$ ) at each location in the incubators was estimated according to Dubinsky (1980) by integrating the product of the spectral irradiance by the phytoplankton spectral absorption coefficient:

$$E_{\text{PUR}} = \int_{\lambda=400}^{700} a_{\text{ph}}(\lambda) E(\lambda) d\lambda. \quad (5)$$

The broadband parameters, the light-limited slope of the photosynthesis–irradiance curve  $\alpha^{\text{B}}$  ( $\text{mg C}(\text{mg Chl})^{-1} \text{h}^{-1}(\mu\text{mol m}^{-2} \text{s}^{-1})^{-1}$ ) and the light saturation parameter  $E_{\text{kPAR}}$  ( $\mu\text{mol m}^{-2} \text{s}^{-1}$ ), which are only given for comparison purpose with values reported previously for other open ocean oligotrophic regions, were obtained by fitting the data to the models of Webb et al. (1974) or Platt et al. (1980) depending if photo-inhibition was observed or not, respectively. Similarly, the photosynthetic parameters for light absorbed by phytoplankton were estimated using the same models.

Without photo-inhibition

$$P_z^{\text{B}} = P_m^{\text{B}} [1 - \exp(-\alpha_{\text{PUR}}^{\text{B}} E_{\text{PUR}} / P_m^{\text{B}})] \quad (6)$$

and with photo-inhibition

$$P_z^{\text{B}} = P_s^{\text{B}} [1 - \exp(-\alpha_{\text{PUR}}^{\text{B}} E_{\text{PUR}} / P_s^{\text{B}})] \times \exp(-\beta_{\text{PUR}}^{\text{B}} E_{\text{PUR}} / P_s^{\text{B}}), \quad (7)$$

where the subscript PUR denotes the light absorbed by phytoplankton ( $\mu\text{mol m}^{-3} \text{s}^{-1}$ ). Because the light-saturated rate of photosynthesis  $P_m^{\text{B}}$  ( $\text{mg C mg Chl}^{-1} \text{h}^{-1}$ ) is wavelength independent (Pickett and Myers, 1966) it can be obtained by fitting the data to broadband or to light absorbed by phytoplankton without distinction.  $P_m^{\text{B}}$  was estimated for the cases with photo-inhibition following Platt et al. (1980) when  $\partial P / \partial E = 0$ . The light saturation parameter for light absorbed by phytoplankton is  $E_{\text{kPUR}} = P_m^{\text{B}} / \alpha_{\text{PUR}}^{\text{B}}$  ( $\mu\text{mol m}^{-3} \text{s}^{-1}$ ).

The maximum quantum yield of carbon fixation ( $\phi_m$ ,  $\text{mol C fixed}(\text{mol photons absorbed})^{-1}$ ) was derived from

$$\phi_m = 0.0231 \text{ Chl } \alpha_{\text{PUR}}^{\text{B}}, \quad (8)$$

where 0.0231 converts milligrams of carbon to moles,  $\mu\text{mol photons}$  to moles and hours to seconds. Note that the units of  $\alpha_{\text{PUR}}^{\text{B}}$  are  $\text{mg C}(\text{mg Chl})^{-1} \text{h}^{-1}(\mu\text{mol m}^{-3} \text{s}^{-1})^{-1}$  because light absorbed by phytoplankton is considered (Eq. (5)).

Daily water-column PP ( $\text{mg C m}^{-2} \text{d}^{-1}$ ) down to the 0.1% surface irradiance depth was estimated at each bio-optical station by combining chlorophyll concentration, hourly spectral light field, the phytoplankton absorption coefficients and the photosynthetic parameters for the light absorbed by phytoplankton. Integration was carried out at hour intervals using the trapezoid rule.

Table 1 shows the main symbols and units used throughout the text.

### 3. Results and discussion

#### 3.1. Hydrographic scenario

The AF, which can be identified by the location of the  $16^\circ\text{C}$  isotherm at  $\sim 200 \text{ m}$  depth (Gould, 1985), was observed at the three large sections A–C (Fig. 3). The transition between northern temperate and subtropical regimes is defined by the region where the  $16^\circ\text{C}$  isotherm uplift is higher (Gould, 1985; Siedler et al., 1985). The elevation of the  $16^\circ\text{C}$  isotherm at stations 30, 14 and 6 in sections C, B and A, respectively, illustrate how the AC meanders as it flows eastward. The

Table 1  
Main symbols, definitions and units used in the text

Symbol	Definition; units
<i>Light</i>	
$a_{zph}(\lambda)$	Phytoplankton spectral absorption coefficient at each depth in the water column; $m^{-1}$
DL	Day length; h
DLS	Day length for saturating conditions of photosynthesis; h
$\bar{E}_{0+}(t)$	Hourly average incident PAR irradiance at the sea surface; $\mu mol m^{-2} s^{-1}$
$\bar{E}_{0+max}$	Maximum incident PAR irradiance at the sea surface; $\mu mol m^{-2} s^{-1}$
$\bar{E}_{0-}(t, \lambda)$	Hourly average spectral irradiance below the sea surface; $\mu mol m^{-2} s^{-1}$
$\bar{E}_z(t, \lambda)$	Hourly average spectral irradiance at each depth in the water column; $\mu mol m^{-2} s^{-1}$
$\bar{E}_{zPUR}(t)$	Hourly average irradiance absorbed by phytoplankton at each depth in the water column; $\mu mol m^{-3} s^{-1}$
$K(\lambda)$	Spectral attenuation coefficient for the water column; $m^{-1}$
<i>Phytoplankton biomass</i>	
Chl	Chlorophyll concentration; $mg m^{-3}$
Chl <sub>DCM</sub>	Integrated chlorophyll concentration at the deep chlorophyll maximum; $mg m^{-2}$
Chl <sub>tot</sub>	Integrated chlorophyll concentration in the photic layer; $mg m^{-2}$
<i>Photosynthesis–irradiance relationships</i>	
$\alpha_{PUR}^B$	Chlorophyll-specific, initial slope for light absorbed by phytoplankton; $mg C (mg Chl)^{-1} h^{-1} (\mu mol m^{-3} s^{-1})^{-1}$
$\beta_{PUR}^B$	Chlorophyll-specific, coefficient of photo-inhibition for light absorbed by phytoplankton; $mg C (mg Chl)^{-1} h^{-1} (\mu mol m^{-3} s^{-1})^{-1}$
$E_{kPUR}$	Light saturation index for light absorbed by phytoplankton; $\mu mol m^{-3} s^{-1}$
$\phi_m$	Maximum quantum yield for carbon fixation; $mol C (mol photons)^{-1}$
$P_m^B$	Chlorophyll-specific, light saturated rate of photosynthesis; $mg C mg Chl^{-1} h^{-1}$
$P_s^B$	Chlorophyll-specific, light saturated rate of photosynthesis in the absence of photo-inhibition; $mg C mg Chl^{-1} h^{-1}$
$P_z^B$	Chlorophyll-specific, photosynthetic rate at each depth in the water column; $mg C mg Chl^{-1} h^{-1}$
<i>Primary production</i>	
PP	Daily water-column primary production; $mg C m^{-2} d^{-1}$
PP <sub>DCM</sub>	Primary production at the deep chlorophyll maximum; $mg C m^{-2} d^{-1}$

horizontal distributions of the thermohaline properties at the surface and at the depth of the DCM ( $\sim 100$  m) illustrate the presence of mesoscale features in the region (Fig. 4). The structure of the AF was clearly perceptible in the distributions of temperature and salinity at the depth of the DCM. Meandering was also evident in the distribution of salinity at the surface but not in that of temperature. North–South gradients of temperature and salinity existed at the depth of the DCM with warmer and saltier water to the South whereas the  $16^\circ C$  isotherm was present at the northeast of the sampling area. This type of North–South gradient also occurred in the salinity distribution at the surface while the temperature distribution showed an

East–West gradient. The seasonal heating of western waters and the influence of colder waters of the NW African upwelling probably modified the general North–South gradient to that observed with colder waters at the eastern side (Fig. 4). We can conclude that the hydrographic situation that we found agrees with that described by Alves and Colin de Verdière (1999), who indicated that the mesoscale structure associated with the AC is developed by the abrupt slope of the thermocline, which results in meanders and eddies at both sides of the AF that give rise to anticyclonic eddies in the north and cyclonic in the south. Further detailed description on the hydrographic field during the cruise can be found in Pérez et al. (2003).

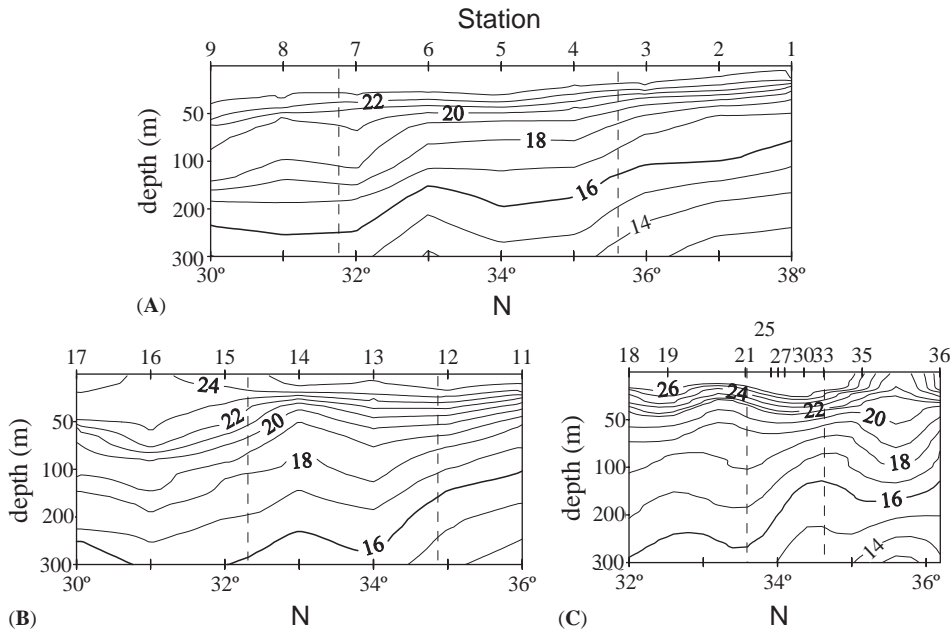


Fig. 3. Vertical distributions of temperature ( $^{\circ}\text{C}$ ) along sections A–C. The upper 100 m has been expanded to show changes in temperature in more detail. Dashed vertical lines delimit the transitional front area between northern and southern regions.

### 3.2. Chlorophyll

Chlorophyll concentrations at the surface were very low ( $<0.1 \text{ mg m}^{-3}$ ), which are characteristic of extremely oligotrophic open ocean waters (Menzel and Ryther, 1960). The DCM was present in the three regions: temperate (North), transitional (AF) and subtropical (South) (Fig. 5), and, as was previously reported for other oligotrophic environments (Cullen and Eppley, 1981), the depth of the DCM was associated with the depth of the nitracline ( $r^2 = 0.76$ , slope = 1.02, nutrient data not shown). The highest Chl concentrations at the DCM ( $\sim 1 \text{ mg Chl m}^{-3}$ ) were found at the southern stations of section C. The other two sections had lower values, with maxima ( $\sim 0.7\text{--}0.8 \text{ mg Chl m}^{-3}$ ) north of the AF region. Chl values in the DCM, south of the AF in section C were considerably higher (5–10 times) than those previously reported for the region during the summer (Fasham et al., 1985; Kahru et al., 1991), when the highest Chl concentrations were found in the temperate waters north of the front. Chl levels in

the DCM were slightly higher than those given by Fernández and Pingree (1996), who also observed enhanced concentrations associated with the AF during early spring.

The depth-integrated Chl concentration (mean  $40 \pm 10 \text{ mg Chl m}^{-2}$ ) in the photic layer for the 17 bio-optical stations (Fig. 6), showed a distribution that reflected the Chl concentration at the DCM (Fig. 5) and the meandering structure of the AF. Chl at the DCM ( $\text{Chl}_{\text{DCM}}$ ) and total integrated Chl ( $\text{Chl}_{\text{tot}}$ ) were related, as would be expected:

$$\text{Chl}_{\text{tot}} = 14.69(\pm 5.06) + 0.95(\pm 0.18)\text{Chl}_{\text{DCM}} \quad (9)$$

$(r^2 = 0.66, P < 0.001)$ ,

where the DCM was defined as the layer that showed a steady increase–decrease in the Chl concentration above and below of the maximum Chl value of the water column.

The DCM accounted for  $67 \pm 13\%$  of total integrated Chl, which was similar to that ( $61.5 \pm 3.5\%$ ) reported by Marañón et al. (2000)

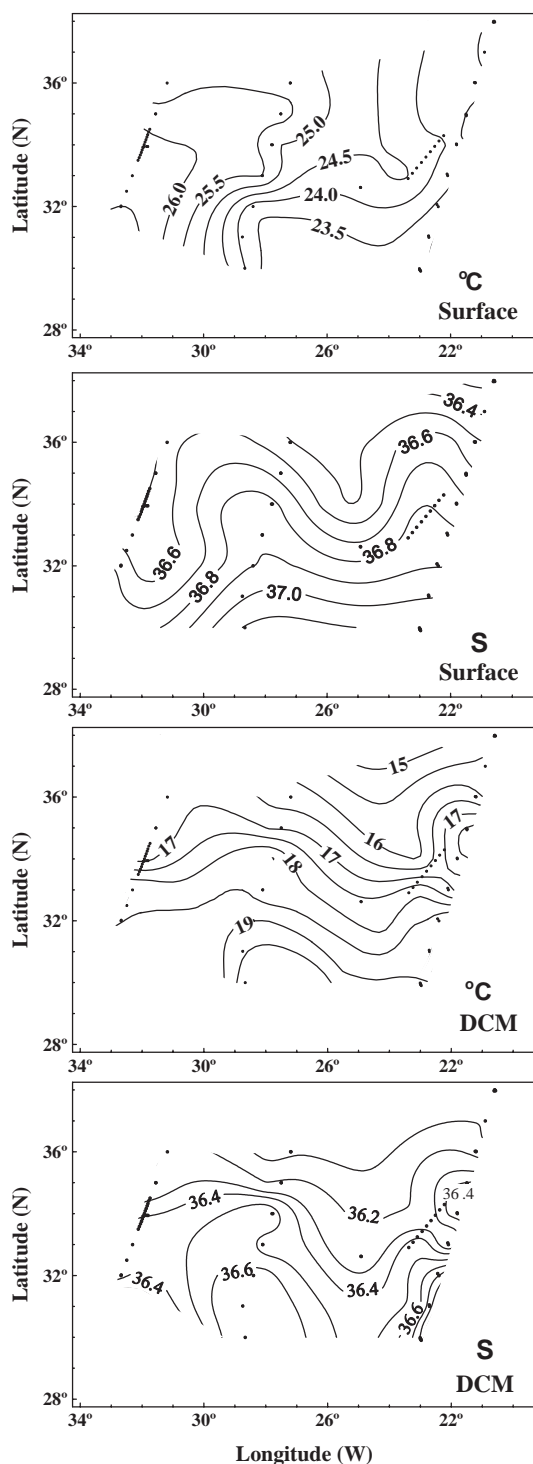


Fig. 4. Horizontal distributions of temperature ( $^{\circ}\text{C}$ ) and salinity (S) at the sea surface and at the depth DCM ( $\sim 100\text{ m}$ ).

over the large-scale AMT-3 section from  $40^{\circ}\text{N}$  to  $40^{\circ}\text{S}$  during September–October 1996.

The highest values ( $> 50\text{ mg Chl m}^{-2}$ ) were found at the northern stations of section A and at both ends of section C, whereas values dropped to  $< 30\text{ mg Chl m}^{-2}$  in the central part of the sampling area (Fig. 6), which coincided with the stronger intrusion of southern waters (Fig. 4) with low Chl levels at the DCM (Fig. 5).

### 3.3. Photosynthetic parameters: vertical variability

The photosynthetic parameters varied with depth at all stations (Fig. 7). The Chl-specific maximum photosynthetic rate ( $P_m^B$ ) and the broadband light saturation parameter ( $E_{kPAR}$ ) decreased with depth from mean values of  $\sim 3\text{ mg C mg Chl}^{-1}\text{ h}^{-1}$  and  $200\ \mu\text{mol m}^{-2}\text{ s}^{-1}$  at the surface to  $< 1\text{ mg C mg Chl}^{-1}\text{ h}^{-1}$  and  $< 30\ \mu\text{mol m}^{-2}\text{ s}^{-1}$  at the depth of the DCM. The broadband light-limited slope ( $\alpha^B$ ) and the maximum quantum yield ( $\phi_m$ ) showed a similar tendency ( $\alpha^B$  vs.  $\phi_m$ ,  $r = 0.95$ ) and increased with depth and mean values below the DCM were  $\sim 4$  times higher than those at the surface.  $P_m^B$  and  $E_{kPAR}$  showed the highest variability at the surface, whereas  $\alpha^B$  and  $\phi_m$  exhibited the least variability. The spectral light saturation parameter  $E_{kPUR}$  did not exhibit such clear tendency as  $E_{kPAR}$  to decrease with depth, although mean value below  $80\text{ m}$  depth was  $\sim 3$  times lower than that above this depth.  $P_m^B$  and  $E_{kPAR}$  were significantly higher ( $P < 0.001$ ) at the surface than at the DCM (Table 2) and  $\alpha^B$  and  $\phi_m$  values were significantly higher at the DCM ( $P < 0.001$ ). There was no significant difference between  $E_{kPUR}$  values at the surface and at the DCM ( $P = 0.09$ ).

This pattern of high  $P_m^B$  and  $E_{kPAR}$  values and low values of  $\alpha^B$  and  $\phi_m$  at the surface, and vice versa at the DCM, is characteristic of stratified oligotrophic seas (Babin et al., 1996; Bouman et al., 2000a) and has been commonly interpreted as photo-acclimation of phytoplankton to the light field in the water column (Falkowski, 1980; Cullen et al., 1992). Higher  $\phi_m$  values at the DCM than at the surface have been attributed to a lower fraction of non-photosynthetic pigments in the phytoplankton at the DCM (Marra et al., 2000; Bouman

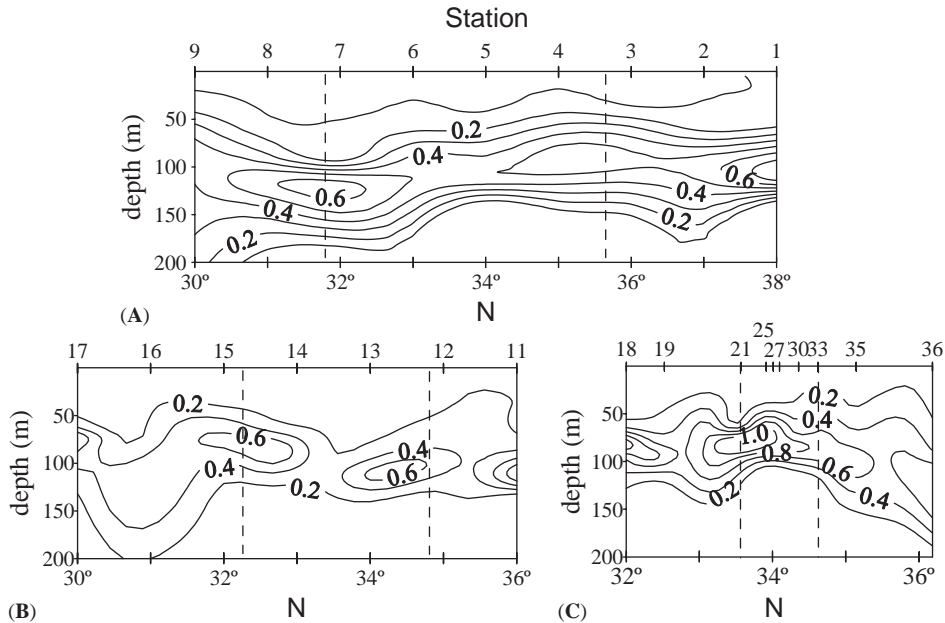


Fig. 5. Vertical distributions of chlorophyll concentration ( $\text{mg Chl m}^{-3}$ ) along sections A–C. Note the difference in intervals. Dashed vertical lines delimit the front between northern and southern regions.

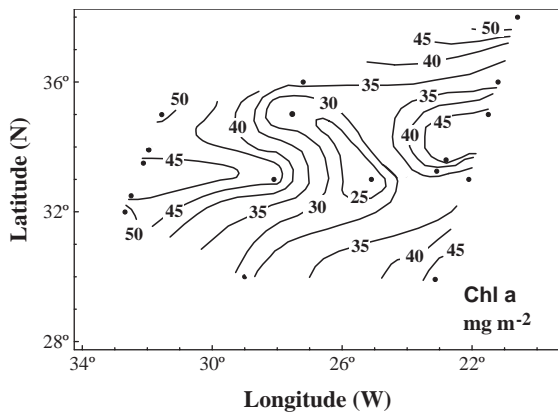


Fig. 6. Horizontal distribution in integrated chlorophyll concentration ( $\text{mg Chl m}^{-2}$ ) in the photic layer.

et al., 2000a), and implies that a high portion of the light absorbed at the DCM is channeled to photosynthesis. Nevertheless, the possible influence of nutrient concentrations on  $\phi_m$  should not be disregarded. Nutrient limitation can also cause low  $\phi_m$  values (Cleveland et al., 1989; Lindley

et al., 1995). In this study, the nitracline was near to the DCM (see above) and  $\phi_m$  values were negatively correlated with the distance from the nitracline ( $r = -0.57$ ,  $P < 0.001$ , depth positive), which can suggest nutrient limitation at the surface waters. In this sense, Babin et al. (1996) showed that both factors (nutrient limitation and contribution of non-photosynthetic pigments) could account for the 50% the variability observed in  $\phi_m$ .

#### 3.4. Photosynthetic parameters: horizontal variability at the surface and at the DCM

When the photosynthetic parameters were analyzed according to the observed horizontal hydrographic gradients (Fig. 4), it was found that there were no significant differences ( $0.17 < P < 0.40$ ) between surface samples to the north and the south of the 36.7 isohaline, which is approximately the center of the salinity gradient at the surface (see Fig. 4). However, significant differences were found in surface samples east and west of the 25°C isotherm, with higher  $P_{\text{ni}}^{\text{B}}$ ,  $\alpha^{\text{B}}$  and  $\phi_m$

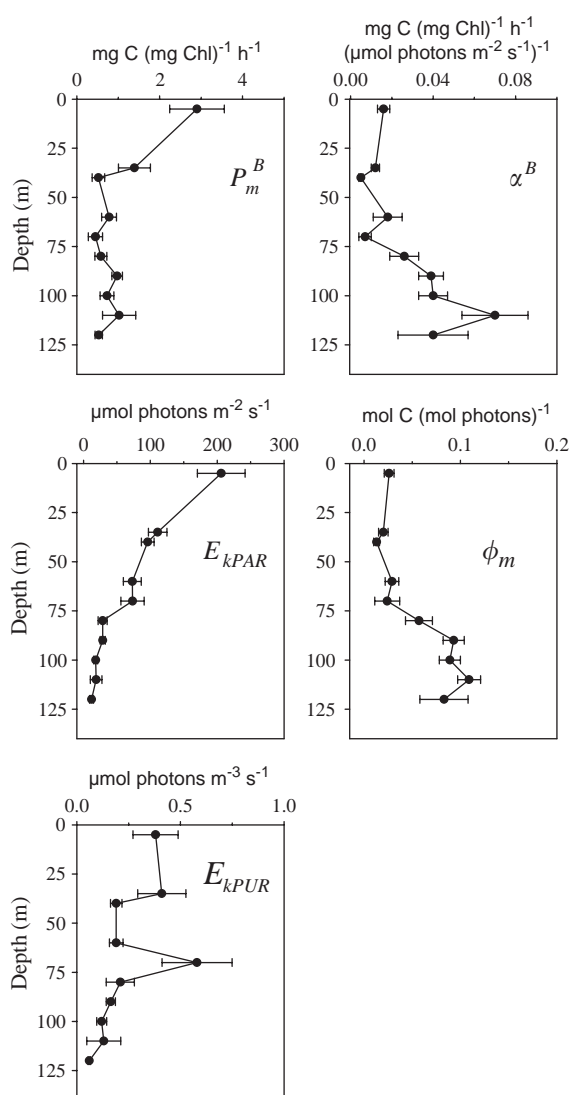


Fig. 7. Mean and standard error vertical profiles for maximum photosynthetic rate  $P_m^B$ , broadband light-limited slope  $\alpha^B$ , light saturation parameter for PAR irradiance  $E_{kPAR}$ , maximum quantum yield  $\phi_m$  and light saturation parameter for light absorbed by phytoplankton  $E_{kPUR}$ .

values ( $P < 0.01$ ) in the western warmer waters (Table 2). In contrast, the broadband and the spectral light saturation parameters were similar at both sides of the 25°C isotherm (Table 2;  $E_{kPAR}$ ,  $P = 0.47$ ;  $E_{kPUR}$ ,  $P = 0.12$ ). This reflects the covariation between  $P_m^B$  and  $\alpha^B$  ( $r = 0.81$ ,  $P < 0.001$ ) and

between  $P_m^B$  and  $\phi_m$  ( $r = 0.77$ ,  $P < 0.01$ ) and also suggests that, although the phytoplankton assemblages at both sides of the front showed different  $P_m^B$ ,  $\alpha^B$  and  $\phi_m$  values, they were acclimated to the rather regular light regime in the region during the cruise (Fig. 2). The highest values of  $P_m^B$  at the surface were found along sections B and C (maximum of 6.35 mg C mg Chl<sup>-1</sup> h<sup>-1</sup> at station 17) whereas section A showed values  $\sim 1.0$  mg C mg Chl<sup>-1</sup> h<sup>-1</sup>. The same pattern was observed in  $\alpha^B$  (maximum value at the surface of 0.036 mg C mg Chl<sup>-1</sup> ( $\mu\text{mol photons m}^{-2} \text{s}^{-1}$ )<sup>-1</sup>) and  $\phi_m$  (maximum of 0.057 mol C (mol photons)<sup>-1</sup>) at station 35 in section C and the lowest values in section A. In the absence of significant variations of light and nutrient concentration, the reactions that determine  $P_m^B$  are strongly influenced by temperature and because surface western waters were warmer than eastern waters, a positive relationship between  $P_m^B$  and temperature would be expected at the surface. However,  $P_m^B$  did not covary with temperature at the surface but was negatively correlated with the depth of the nitracline ( $r = -0.56$ ,  $P < 0.05$ , depth positive), which suggests that nutrient supply from below the nitracline may exert a control on variations of  $P_m^B$ . Negative relationships between  $P_m^B$  and depth of the nitracline have also been reported in other studies (e.g. Marañón and Holligan, 1999). Despite significant correlations between  $\alpha^B$  and  $\phi_m$  with  $P_m^B$ , the correlation between  $\alpha^B$  and  $\phi_m$  at the surface with the depth of the nitracline was not significant. The range of variation found in values of  $P_m^B$ ,  $\alpha^B$  and  $\phi_m$  at the surface in western and eastern waters at the AF region was similar to that reported over larger spatial scales (Keywalyanga et al., 1998; Marañón and Holligan, 1999) and highlights the importance of accurate characterization and resolution of spatial variability of photosynthetic parameters for their application in PP models (e.g. Morel et al., 1996).

By contrast, there were no differences ( $0.10 < P < 0.91$ ) between the photosynthetic parameters at the northern, frontal and southern waters at the depth of the DCM (Table 2), which is probably consequence of phytoplankton acclimation to the relatively stable conditions at this depth (Venrick, 1982).

Table 2

Mean and standard deviations of  $P_m^B$  ( $\text{mg C}(\text{mg Chl})^{-1}\text{h}^{-1}$ ),  $\alpha_m^B$  ( $\text{mg C}(\text{mg Chl})^{-1}\text{h}^{-1}(\mu\text{mol m}^{-2}\text{s}^{-1})^{-1}$ ),  $E_{kPAR}$  ( $\mu\text{mol m}^{-2}\text{s}^{-1}$ ),  $\phi_m$  ( $\text{mol C}(\text{mol photons})^{-1}$ ) and  $E_{kPUR}$  ( $\mu\text{mol m}^{-3}\text{s}^{-1}$ ) at the surface and at the DCM and for different domains in the Azores Front

Layer	Domains	$P_m^B$	$\alpha_m^B$	$E_{kPAR}$	$\phi_m$	$E_{kPUR}$
Surface	Total	$2.90 \pm 2.47$	$0.016 \pm 0.012$	$206 \pm 134$	$0.026 \pm 0.019$	$0.38 \pm 0.43$
DCM	Total	$0.88 \pm 0.60$	$0.044 \pm 0.024$	$28 \pm 20$	$0.091 \pm 0.038$	$0.20 \pm 0.17$
Surface	West	$4.09 \pm 2.37$	$0.024 \pm 0.011$	$175 \pm 87$	$0.040 \pm 0.015$	$0.21 \pm 0.12$
Surface	East	$0.93 \pm 0.30$	$0.006 \pm 0.004$	$234 \pm 186$	$0.009 \pm 0.008$	$0.58 \pm 0.57$
DCM	North	$1.11 \pm 0.85$	$0.041 \pm 0.025$	$32 \pm 18$	$0.095 \pm 0.039$	$0.20 \pm 0.14$
DCM	Front	$0.58 \pm 0.30$	$0.043 \pm 0.031$	$28 \pm 29$	$0.076 \pm 0.043$	$0.22 \pm 0.25$
DCM	South	$0.99 \pm 0.39$	$0.050 \pm 0.019$	$21 \pm 10$	$0.109 \pm 0.024$	$0.18 \pm 0.08$

Note: West and East waters were separated at the surface by the 25°C isotherm. North, Front and South regions were by the uplift of the 16°C isotherm in sections A–C (see Fig. 3).

### 3.5. Primary production

Daily water-column PP (mean  $346 \pm 170 \text{ mg C m}^{-2} \text{ d}^{-1}$ ) ranged from 173 to  $664 \text{ mg C m}^{-2} \text{ d}^{-1}$ . The meandering structure of the AF with intrusions of several other water bodies with different photo-physiology characteristics has an influence on the resulting PP (Fig. 8). The lowest values ( $< 200 \text{ mg C m}^{-2} \text{ d}^{-1}$ ) occurred east of the sampling area, where the photosynthetic parameters at the surface were lower. The highest PP values ( $> 500\text{--}600 \text{ mg C m}^{-2} \text{ d}^{-1}$ ) were recorded toward west and at the northern part of section B where photosynthetic parameters were higher at the surface. PP was also  $> 500 \text{ mg C m}^{-2} \text{ d}^{-1}$  at station 41 (see Fig. 1) where there was an influence from northern waters (see Fig. 4). These PP values were slightly higher than the values reported by Jochem and Zeitzschle (1993) at 33°N, 21°W during the post spring bloom ( $0.1\text{--}0.35 \text{ g C m}^{-2} \text{ d}^{-1}$ ) and were similar to those determined during summer ( $0.26 \text{ g C m}^{-2} \text{ d}^{-1}$ ) by Frazel and Berberian (1990). In contrast, they were lower than the values measured at 26°W ( $0.3\text{--}0.9 \text{ g C m}^{-2} \text{ d}^{-1}$ ) during spring by Fernández and Pingree (1996).

PP at the DCM (mean  $178 \pm 88 \text{ mg C m}^{-2} \text{ d}^{-1}$ ) represented a significant fraction ( $54 \pm 17\%$ ) of the total integrated PP and 71% of the variability in PP could be explained by a single linear relationship with PP at the DCM. The explained variability increased to 92% when  $P_m^B$  at the

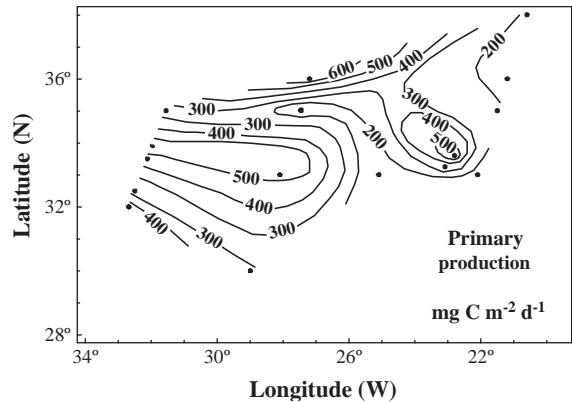


Fig. 8. Distribution of daily depth-integrated PP ( $\text{mg C m}^{-2} \text{ d}^{-1}$ ). Station 9 was omitted because of very low carbon fixation signature in the surface layer.

surface was included in the relationship

$$PP = 35.02(\pm 6.73)P_m^B + 1.58(\pm 0.21)PP_{DCM} \quad (r^2 = 0.91, P < 0.001) \quad (10)$$

which indicates that an additional 20% of the variability in PP was caused by variations in PP at the surface layers associated with the East–West variability in  $P_m^B$  values. Marañón and Holligan (1999) also found that variations in  $P_m^B$  at the surface could account for 30% of the variability of PP in two large-scale AMT transects between 50°N and 50°S.

### 3.6. Photosynthesis and light regime in the water column: is carbon uptake light-limited?

The case that we present here for the AF region during summer, where PP at the DCM was responsible for a half of the total PP and caused 71% of its variability, provides an opportunity to assess the influence of light limitation at the deepest layers of the photic zone.

To investigate if light limitation occurs in the AF region, daily mean light absorbed by phytoplankton ( $\bar{E}_{zPUR}$ ) was compared with the corresponding spectral light saturation parameter ( $E_{kPUR}$ ) for the photic layer and for the DCM in particular. Light limitation will occur when  $\bar{E}_{zPUR} < E_{kPUR}$  (Figueiras et al., 1999). Photic layer and DCM mean values of these two variables are given in Table 3.  $\bar{E}_{zPUR}$  was significantly higher than  $E_{kPUR}$  in the photic layer but there was no significant difference between  $\bar{E}_{zPUR}$  and  $E_{kPUR}$  at the DCM. This could imply that photosynthesis was not light-limited in the whole photic layer.

Therefore, if photosynthesis was not light-limited, PP computed considering the whole spectral resolution should be equal to PP estimated according to

$$PP = DL \int_{Z=0}^{Z_{0.1\%}} P_m^B(z) \text{Chl}(z) dz, \quad (11)$$

where DL is the day length in hours (15h). However, PP computed using Eq. (11) was overestimated by  $\sim 77\%$  (Fig. 9), which indicates that light limitation should be actually occurring at some depths and/or light hours. An examination of hourly pair values of  $E_{zPUR}$  and  $E_{kPUR}$  showed that photosynthesis was light-limited

Table 3

Mean and standard deviations in the photic layer and at the DCM for the spectral light saturation parameter  $E_{kPUR}$  ( $\mu\text{mol m}^{-3} \text{s}^{-1}$ ) and daily mean light absorption by phytoplankton  $\bar{E}_{zPUR}$  ( $\mu\text{mol m}^{-3} \text{s}^{-1}$ )

Layer	$E_{kPUR}$	$\bar{E}_{zPUR}$	$P$
Photic layer	$0.24 \pm 0.27$	$0.71 \pm 0.76$	$< 0.001$
DCM	$0.20 \pm 0.17$	$0.21 \pm 0.13$	0.96

Note:  $P$  values are the probabilities of  $t$ -tests for paired samples.

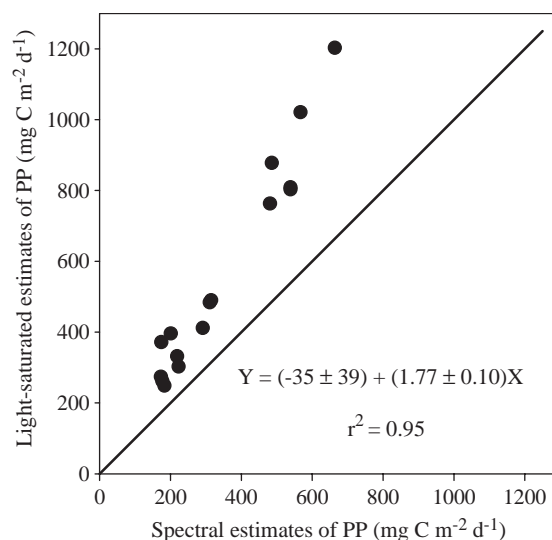


Fig. 9. Spectral vs. light-saturated estimates of PP. Light-saturated estimates of PP were made using Eq. (11). See more details in text. Equation inside is for model II of the linear regression. Solid line corresponds to the 1:1 relationship.

( $E_{zPUR}/E_{kPUR} < 1$ ) at dawn and dusk at all stations, with limitation lasting for longer periods of time at the DCM (Fig. 10). For all stations, carbon fixed under light-limited conditions occurred during 47% of the time. A similar situation has also been observed by Morel et al. (1996) in oligotrophic regions.

This interpretation could be biased due to the photoadaptation that phytoplankton undergoes during 2–3 h incubations (Lewis and Smith, 1983; Lewis et al., 1984; Lizon and Lagadeuc, 1995), which mainly occurs through changes in the maximum photosynthetic rate and the initial slope resulting in higher values of the light saturation index than in those obtained with shorter (20–30 min) incubations. If this photoadaptation took place during our incubations, therefore, the  $E_{kPUR}$  values should be in fact lower and, consequently, the periods of time and places with light limitation ( $E_{zPUR}/E_{kPUR} < 1$ ) should be actually less.

Because light limitation seems to be important in this region, the light influence on carbon fixation was further analyzed by re-computing spectral PP under different levels of incident irradiance (Fig. 11). PP varied little and slowly for irradiance levels above 50% of the actual

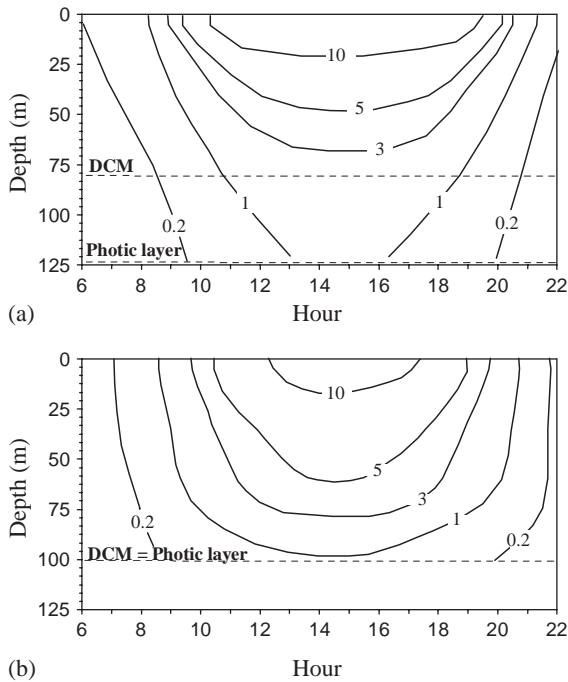


Fig. 10. Time and depth distribution of the ratio between the light absorbed by phytoplankton and the light saturation parameter for the light absorbed by phytoplankton ( $E_{zPUR}/E_{kPUR}$ ) for two contrasting stations, station 35 (A) and station 17 (B). In (A) the DCM is within the photic layer and in (B) the DCM is located at the bottom of the photic layer. The mean incident irradiance at the surface (Fig. 2) and the  $E_{kPUR}$  values from P–E determinations were used to derive these ratios.

value, where PP was still 82%. The level of incident irradiance, analogous to the light saturation parameter, below which PP diminished noticeably was  $18 \text{ mol m}^{-2} \text{ d}^{-1}$  (34% of the actual incident irradiance) and corresponded with a PP value of  $232 \text{ mg C m}^{-2} \text{ d}^{-1}$  (67% of the actual value). PP changes were especially low (maximum change 6%) at irradiances between 80% and 130% of the actual value. These slight variations in PP caused by significant changes of incident irradiance above the actual value suggest that production during the light-limited hours at dawn and dusk (Fig. 10) was a small fraction of the total production; otherwise higher increases of PP should be expected. To assess this, PP was computed using Eq. (11) but substituting the day length DL (15 h) with *the day length for saturating*

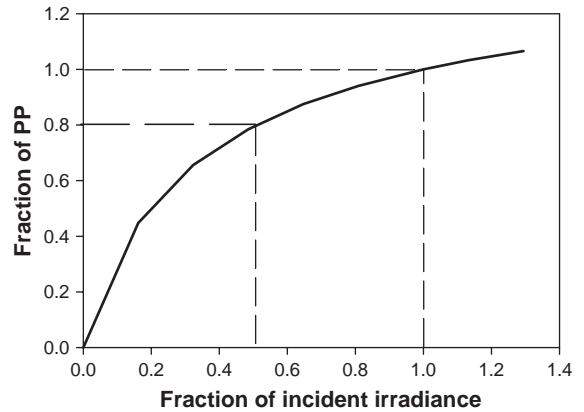


Fig. 11. Fraction of the reference value of spectral PP as a function of fraction of incident irradiance. Actual values are represented by 1. Values of the fraction of PP are the average of 17 stations. The reference values and those corresponding to 50% of the incident irradiance are represented by dashed lines.

conditions DLS when  $E_{zPUR}/E_{kPUR} > 1$  (8 h, which is 53% of the DL). Good coincidence was obtained between PP calculated using Eq. (11) with DLS and that estimated with spectral resolution (Fig. 12), which further suggests that production under light-limited hours was a low part of the total PP. This is explained by the photosynthetic response of phytoplankton at the DCM, where more than a half of PP took place and light limitation was stronger. The high maximum quantum yields and the low maximum photosynthetic rates (Table 2) determine that carbon fixation moves from near zero to saturated values and vice versa very quickly during changes in irradiance during sunrise and sunset.

Although this result was obtained without considering the diel variability in photosynthesis and remains untested in other oligotrophic regions of the ocean and at different seasons, this method offers an accurate and simple tool for estimating PP in this area. Whereas spectral models require accurate measurements or estimates of many variables, including the variability in maximum quantum yield, Eq. (11) only requires modeling vertical profiles of  $P_m^B$  and chlorophyll, because *the day length for saturating* conditions DLS can be easily estimated by dividing the total incident irradiance during day light hours by the maximum

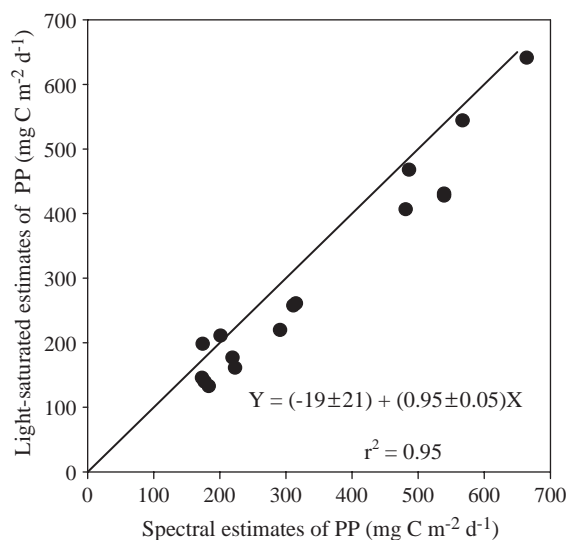


Fig. 12. Spectral vs. light-saturated estimates of PP calculated using Eq. (11) but substituting the day length DL for *the day length for saturating irradiance* DLS. Further details are given in the text. Equation inside is for model II of the linear regression. Solid line corresponds to the 1:1 relationship.

incident irradiance when photosynthesis is saturated:

$$DLS = \frac{\int_{t=\text{sunrise}}^{\text{sunset}} \bar{E}_{0+}(t) dt}{\bar{E}_{0+\max}} \quad (12)$$

There has been considerable progress in predicting vertical profiles of chlorophyll (e.g. Platt and Sathyendranath, 1988; Morel and Berthon, 1989) and modeling  $P_m^B$  commences to be successful (Behrenfeld et al., 2002a, b), which will ultimately add to the utility of the DLS model to estimate integrated PP. However, as it has been recognized by Behrenfeld et al. (2002b), spectrally resolved models are still necessary to estimate acclimation irradiances in the water column.

#### 4. Conclusions

While the vertical variability of the photosynthetic parameters in the heterogeneous region of the Azores Front during summer was that typical of oligotrophic waters, the horizontal variability at the surface was similar to that found over larger spatial scales in the Atlantic Ocean. Integrated

primary production varied by a factor of 4 with 91% of this variability due to variations in primary production at the deep chlorophyll maximum (71%) and the maximum photosynthetic rate ( $P_m^B$ ) at the surface waters (20%). Despite the fact that photosynthesis was light-limited in the photic layer at dawn and dusk, primary production could be accurately estimated by a simple light-saturated model that considers chlorophyll-specific maximum photosynthetic rate ( $P_m^B$ ) and chlorophyll concentration in the photic layer and the day length equivalent to saturating irradiance of photosynthesis. This suggests that modeling primary production in stratified oceans with permanent DCM could be greatly simplified by ignoring the spectral resolution and indicates that further effort should be focused on characterizing and predicting the spatial and temporal variations in chlorophyll-specific maximum photosynthetic rates in these vast oligotrophic oceanic regions.

#### Acknowledgements

We thank the personnel aboard R./V. *BIO Hespérides* during the AZORES I cruise. Special thanks to Dr. Noga Stambler for help with the absorption spectra, to Dr. Eduardo Pérez for light measurements and to Pilar Pazos for help with ship borne determinations of photosynthetic parameters. L.M.L. was supported by a fellowship from the Spanish Ministerio de Educación y Ciencia. I.M. was funded by a fellowship from Caixanova. This research was supported by the EU CANIGO project (MAS3-CT96-0060).

#### References

- Alves, M.L.G.R., Colin de Verdière, A., 1999. Instability dynamics of a subtropical jet and applications to Azores Fronts Current System: eddy-driven mean flow. *Journal of Physical Oceanography* 29, 837–864.
- Arbones, B., Figueiras, F.G., Zapata, M., 1996. Determination of phytoplankton absorption coefficient in natural seawater samples: evidence of a unique equation to correct the pathlength amplification on glass-fiber filters. *Marine Ecology Progress Series* 137, 293–304.

- Arbones, B., Figueiras, F.G., Varela, R., 2000. Action spectrum and maximum quantum yield of carbon fixation in natural phytoplankton populations: implications for primary production estimates in the ocean. *Journal of Marine Systems* 26, 97–114.
- Babin, M., Morel, A., Claustre, H., Bricaud, A., Kolber, Z., Falkowski, P.G., 1996. Nitrogen and irradiance dependent variations of maximum quantum yield of carbon fixation in eutrophic, mesotrophic and oligotrophic marine systems. *Deep-Sea Research I* 43, 1241–1272.
- Behrenfeld, M.J., Falkowski, P.G., 1997a. Photosynthetic rates derived from satellite-based chlorophyll concentration. *Limnology and Oceanography* 42, 1–20.
- Behrenfeld, M.J., Falkowski, P.G., 1997b. A consumer's guide to phytoplankton primary productivity models. *Limnology and Oceanography* 42, 1479–1491.
- Behrenfeld, M.J., Marañón, E., Siegel, D.A., Hooker, S.B., 2002a. Photoacclimation and nutrient-based model of light-saturated photosynthesis for quantifying oceanic primary production. *Marine Ecology Progress Series* 228, 103–117.
- Behrenfeld, M.J., Esaias, W.E., Turpie, K.R., 2002b. Assessment of primary production at the global scale. In: Williams, P.J.leB., Thomas, D.N., Reynolds, C.S. (Eds.), *Phytoplankton Productivity. Carbon Assimilation in Marine and Freshwater Ecosystems*. Blackwell Science, Oxford, pp. 156–186.
- Bouman, H.A., Platt, T., Kraay, G.W., Sathyendranath, S., Irwin, D.B., 2000a. Bio-optical properties of the subtropical North Atlantic. I. Vertical variability. *Marine Ecology Progress Series* 200, 3–18.
- Bouman, H.A., Platt, T., Sathyendranath, S., Irwin, D.B., Wernard, M.R., Kraay, G.W., 2000b. Bio-optical properties of the subtropical North Atlantic. II. Relevance to models of primary production. *Marine Ecology Progress Series* 200, 19–34.
- Cleveland, J.S., Perry, M.J., Kiefer, D.A., Talbot, M.C., 1989. Maximum quantum yield of photosynthesis in the north-western Sargasso Sea. *Journal of Marine Research* 47, 869–889.
- Cullen, J.J., 1982. The deep chlorophyll maximum: comparing vertical profiles of chlorophyll *a*. *Canadian Journal of Fisheries and Aquatic Sciences* 39, 791–803.
- Cullen, J.J., Eppley, R.W., 1981. Chlorophyll maximum layers of the southern California Bight and possible mechanisms of their formation and maintenance. *Oceanologica Acta* 4, 23–32.
- Cullen, J.J., Lewis, M.R., Davis, C.O., Braber, R.T., 1992. Photosynthetic characteristics and estimated growth rates indicate grazing is the proximate control of primary production in the equatorial Pacific. *Journal of Geophysical Research* 97, 639–654.
- Dubinsky, Z., 1980. Light utilization efficiency in natural phytoplankton communities. In: Falkowski, P.G. (Ed.), *Primary Productivity in the Sea*. Plenum, New York, pp. 83–97.
- Falkowski, P.G., 1980. Light-shade adaptation in marine phytoplankton. In: Falkowski, P.G. (Ed.), *Primary Productivity in the Sea*. Plenum, New York, pp. 99–120.
- Fasham, M.J.R., Platt, T., Irwin, B., Jones, K., 1985. Factors affecting the spatial pattern of the deep chlorophyll maximum in the region of the Azores Front. *Progress in Oceanography* 14, 129–165.
- Fernández, E., Pingree, R.D., 1996. Coupling between physical and biological fields in the North Atlantic subtropical front southeast of the Azores. *Deep-Sea Research I* 43, 1369–1393.
- Figueiras, F.G., Arbones, B., Estrada, M., 1999. Implications of bio-optical modeling of phytoplankton photosynthesis in Antarctic waters: further evidence of no light limitation in the Bransfield Strait. *Limnology and Oceanography* 44, 1599–1608.
- Frazel, D.W., Berberian, G., 1990. Distributions of chlorophyll and primary productivity in relation to water column structure in the eastern North Atlantic Ocean. *Global Biogeochemical Cycles* 4, 241–251.
- González, N., Anadón, R., Mouriño, B., Fernández, E., Sinha, B., Escáñez, J., de Armas, D., 2001. The metabolic balance of the planktonic community in the North Atlantic Subtropical Gyre: the role of mesoscale instabilities. *Limnology and Oceanography* 46, 946–952.
- Gould, W.J., 1985. Physical oceanography of the Azores Front. *Progress in Oceanography* 14, 167–190.
- Jochem, F., Zeitzschle, B., 1993. Productivity regime and phytoplankton size structure in the tropical and subtropical North Atlantic in spring 1989. *Deep-Sea Research I* 40, 495–519.
- Kahru, M., Nomman, S., Zeitzschel, B., 1991. Particle (plankton) size structure across the Azores Front (Joint global ocean flux study North Atlantic bloom experiment). *Journal of Geophysical Research* 96, 7083–7088.
- Käse, R.H., Siedler, G., 1982. Meandering of the subtropical front, south-east of Azores. *Nature* 300, 245–246.
- Keywalyanga, M.N., Platt, T., Sathyendranath, S., 1992. Ocean primary production calculated by spectral and broad band models. *Marine Ecology Progress Series* 85, 171–185.
- Keywalyanga, M.N., Platt, T., Sathyendranath, S., Lutz, V.A., Stuart, V., 1998. Seasonal variations in physiological parameters of phytoplankton across the North Atlantic. *Journal of Plankton Research* 20, 17–42.
- Kirk, J.T.O., 1983. *Light and Photosynthesis in Aquatic Ecosystems*. Cambridge University Press, Cambridge, 401pp.
- Kishino, M., Takahashi, M., Okami, N., Ichimura, S., 1985. Estimation of the spectral absorption coefficients of phytoplankton in the sea. *Bulletin of Marine Sciences* 37, 634–642.
- Klein, B., Siedler, G., 1989. On the origin of the Azores Current. *Journal of Geophysical Research* 94, 6159–6168.
- Lewis, M.R., Smith, J.C., 1983. A small volume, short-incubation-time method for measurement of photosynthesis as a function of incident irradiance. *Marine Ecology Progress Series* 13, 99–102.

- Lewis, M.R., Cullen, J.J., Platt, T., 1984. Relationships between vertical mixing and photoadaptation of phytoplankton: similarity criteria. *Marine Ecology Progress Series* 15, 141–149.
- Lindley, S.T., Bidigare, R.R., Barber, R.T., 1995. Phytoplankton photosynthesis parameters along 140°W in the equatorial Pacific. *Deep-Sea Research II* 42, 441–463.
- Lizon, F., Lagadeuc, Y., 1995. Echelles temporelles et production primaire: considérations méthodologiques. *Journal de Recherche Océanographique* 20, 84–88.
- Marañón, E., Holligan, P.M., 1999. Photosynthetic parameters of phytoplankton from 50°N to 50°S in the Atlantic Ocean. *Marine Ecology Progress Series* 176, 191–203.
- Marañón, E., Holligan, P.M., Varela, M., Mouriño, B., Bale, A.J., 2000. Basin scale variability of phytoplankton biomass, production and growth in the Atlantic Ocean. *Deep-Sea Research I* 47, 825–857.
- Marra, J., Trees, C.C., Bidigare, R.R., Barber, R.T., 2000. Pigment absorption and quantum yields in the Arabian Sea. *Deep-Sea Research II* 47, 1279–1299.
- Menzel, D.W., Ryther, J.H., 1960. The annual cycle of primary production in the Sargasso Sea off Bermuda. *Deep-Sea Research* 6, 351–367.
- Moore, L.R., Goericke, R., Chisholm, S.W., 1995. Comparative physiology of *Synechococcus* and *Prochlorococcus*: influence of light and temperature on growth, pigments, fluorescence and absorptive properties. *Marine Ecology Progress Series* 116, 259–275.
- Morel, A., 1991. Light and marine photosynthesis: a spectral model with geochemical and climatological implications. *Progress in Oceanography* 26, 263–306.
- Morel, A., Berthon, J.F., 1989. Surface pigments, algal biomass profiles, and potential production of the euphotic layer: relationships reinvestigated in view of remote-sensing applications. *Limnology and Oceanography* 34, 1545–1562.
- Morel, A., Antoine, D., Babin, M., Dandonneau, Y., 1996. Measured and modeled primary production in the northeast Atlantic (EUMELI JGOFS program): the impact of natural variations in photosynthetic parameters on model predictive skill. *Deep-Sea Research I* 43, 1273–1304.
- Pérez, F.F., Gilcoto, M., Ríos, A.F., 2003. Large and mesoscale variability of the water masses and the deep chlorophyll maximum in the Azores Front. *Journal of Geophysical Research* 108, 3215–3233.
- Pickett, J.M., Myers, J., 1966. Monochromatic light saturation curves for photosynthesis in *Chlorella*. *Plant Physiology* 41, 90–98.
- Pingree, R.D., 1997. The eastern subtropical gyre (North Atlantic): flow rings recirculations structure and subduction. *Journal Marine Biological Association, UK* 77, 573–624.
- Platt, T., Sathyendranath, S., 1988. Oceanic primary production: estimation by remote sensing at local and regional scales. *Science* 241, 1613–1620.
- Platt, T., Gallegos, C.L., Harrison, W.G., 1980. Photoinhibition of photosynthesis in natural assemblages of marine phytoplankton. *Journal of Marine Research* 38, 687–701.
- Platt, T., Subba Rao, D.V., Irwin, B., 1983. Photosynthesis of picoplankton in the oligotrophic ocean. *Nature* 301, 702–704.
- Siedler, G., Zenk, W., Emery, W.J., 1985. Strong currents events related to a subtropical front in the northeast Atlantic. *Journal of Physical Oceanography* 19, 1208–1221.
- Venrick, E.L., 1982. Phytoplankton in an oligotrophic ocean: observations and questions. *Ecological Monographs* 52, 129–154.
- Webb, W.L., Newton, M., Starr, D., 1974. Carbon dioxide exchange of *Alnus rubra*: a mathematical model. *Oecologia* 17, 281–291.